Advances in Environmental Research, *Vol. 5, No. 4 (2016) 263-282*
DOI: https://doi.org/10.12989/aer.2016.5.4.263

Development a numerical model of flow and contaminant transport in layered soils

Hossein Ahmadi[1], Masoud M. Namin[1] and Fouad Kilanehei[*2]

[1]*Department of Civil Engineering, University of Tehran, Tehran, Iran*
[2]*Department of Civil Engineering, Imam Khomeini International University, Qazvin, Iran*

(Received November 1, 2016, Revised January 9, 2017, Accepted January 10, 2017)

Abstract. Contaminant transport in groundwater induces major threat and harmful effect on the environment; hence, the fate of the contaminant migration in groundwater is seeking a lot of attention. In this paper a two dimensional numerical flow and transport model through saturated layered soil is developed. Groundwater flow and solute transport has been simulated numerically using proposed model. The model implements the finite volume time splitting method to discretize the main equations. The performance, accuracy and efficiency of the out coming numerical models have been successfully examined by two test cases. The verification test cases consist of two-dimensional, groundwater flow and solute transport. The final purpose of this paper is to discuss and compare the shape of contaminant plume in homogeneous and heterogeneous media with different soil properties and control of solute transport using a zone for minimizing the potential of groundwater contamination; furthermore, this model leads to select the effective and optimum remedial strategies for cleaning the contaminated aquifers.

Keywords: groundwater flow; solute transport; finite volume method; time splitting method; layered soils

1. Introduction

Throughout 20th century, wide range of environmental problems caused by contaminants was frequently reported around the world. Groundwater polluted by hyper saline water in arid or semi-arid area (Boufadel *et al*. 1999), contaminant leakage in landfills and waste disposal at urban areas, (El-Zein 2008, Zhang and Schwartz 1995), and seawater intrusion in coastal area (Zhang *et al.* 2002), are important cases in point; thus, there is a growing concern over contaminant migration problems especially in subsurface systems. Contaminant transport by flowing water has broad impact in environmental protection and resource utilization. The leaching of salts and nutrients in soils also has considerable influence on agricultural production (Bear and Cheng 2010). The management of polluted subsurface systems for control of groundwater quality will be a vital requirement for sustainability. The effective management of contaminated aquifers and the selection of proper and effective remedial technologies depend on the accurate and precise simulation and prediction of flow and solute transport. In order to investigate contaminant

∗Corresponding author, Assistant Professor, E-mail: kilanehei@eng.ikiu.ac.ir

http://www.techno-press.org/?journal=aer&subpage=7 ISSN: 2234-1722 (Print), 2234-1730 (Online)

transport in groundwater systems, mathematical modeling should be developing. Nevertheless, some analytical solutions in last decade were introduced (Li and Cleall 2011, Abolbashari *et al*. 2016), these solutions to such problems with complex geometry and complicated boundary conditions, are almost impossible to obtain; as a result, it brings about numerical modeling becomes the method of choice for analyzing contaminant transport through the subsurface media (McDonald and Harbaugh 1988). Solving transport equation requires the knowledge of velocity distribution throughout the solution domain; consequently, for meeting this requirement, mathematical models should be based on the governing flow equation.

Flow simulation in porous media has been extensively studied in last decades for determining the groundwater properties. A proper description of contaminant transport plays a major role in many aqueous systems. For subsurface flows, description of the transport physics must often be augmented by chemical and/or biological considerations. This generally leads to advective-diffusive-reactive transport equations. The solution of this equation is a long standing problem and many numerical methods have been introduced to model accurately the interaction between advective, diffusive and reactive processes. In recent field studies, there is an increasing interest in solving together flow and solute transport in underground water.

The mathematical nature of the flow and transport equations has different and specific methods for their approximations in numerical simulation. In general, the numerical solution of flow and transport equations has been dominated by finite difference, finite element and finite volume.
Finite difference method broadly is used for solving partial differential groundwater equation as one the oldest method (Igboekwe and Achi 2011). Hulagabali *et al.* (2014), Jobson and Harbaugh (1999) can be counted as a few samples among many other works in the advection-diffusion equations. In addition to this classical approach, there is finite element method, which has been widely used for solving flow equation in the last two decades (Satavalekar and Sawant 2014). In compare to finite difference method this method provides an appropriate geometric flexibility. Furthermore, this method is also another application to use an accurate approximation for ADR equation (Sudicky 1989). Sirvastava and Yeh (1992) presented a Galerkin finite element method for modelling water and transport of chemically reactive solute through porous media under variably saturated conditions. Other more recent techniques such as either mesh less numerical method based on smoothed particle hydrodynamics (SPH) (Herrera *et al*. 2009) and mesh free method (Khoshghalb and Khalili 2013) was introduced in the recent investigation.

A limited amount of research is undertaking regard to the fate of the contaminant in layered soil and the effect of zone on the controlling of pollution migration. In the present investigation, an attempt has been made to provide a simple but sufficiently accurate numerical modeling of the two dimensional solute transport through the saturated layered soils using finite volume method in order to explore the shape of contaminant plume.

2. Governing equation

The groundwater flow is simulated by combination of Darcy's law and mass conservation equation, yielding the Boussinesq' equation and the solute transport is described by the advection-dispersion-reactive equation.

2.1 Equation for flow in saturated media

The following equation is taken as the equation governing three dimensional flow of groundwater in saturated porous media (Bear 1979)

$$S_s \frac{\partial h}{\partial t} = \nabla.(K.\nabla h) \tag{1}$$

Where K is the hydraulic conductivity; h is hydraulic head; S_s is specific storage and t is time.
Eq. (1) can be written in two dimensional as

$$S_s \frac{\partial h}{\partial t} = \frac{\partial}{\partial x}(K_x \frac{\partial h}{\partial x}) + \frac{\partial}{\partial z}(K_z \frac{\partial h}{\partial z}) \tag{2}$$

2.2 Equations for transport of contaminants

The solute transport mathematical model is presented with the following equation (Bear 1979)

$$R_d \frac{\partial C}{\partial t} = \nabla.(D\nabla C) - \nabla.(v_a C) - \lambda R_d C \tag{3}$$

Eq. (3) can be written in two dimensional as

$$R_d \frac{\partial C}{\partial t} = \frac{\partial}{\partial x}(D_x \frac{\partial C}{\partial x}) + \frac{\partial}{\partial z}(D_z \frac{\partial C}{\partial z}) - \frac{\partial (v_{ax} C)}{\partial x} - \frac{\partial (v_{az} C)}{\partial z} - \lambda R_d \tag{4}$$

Where D is the hydrodynamic dispersion coefficient; v is the seepage velocity; C is the contaminant concentration; λ is the decay constant and R_d is the retardation factor (Bear 1979)

$$R_d = (1 + \frac{\rho_b}{n} N K_d C^{N-1}) \tag{5}$$

Where ρ_b is the bulk density of contaminant and K_d is distribution coefficient.
The first term on the right side of Eq. (4) represents the change in concentration due to hydrodynamic dispersion. The second term represents advective transport, and describes the movement of solutes at seepage velocity of the flowing groundwater. The third term lumps all of the chemical, geochemical, and biological reactions that cause transfer of mass between the liquid and solid phases or conversion of dissolved chemical species from one form to another.

3. Transport contamination mechanism

The mechanism of the pollution migration in porous media generally has two major parts. One of them is, physical processes move mass from point to point and the second one is chemical and biological process redistributes mass. This mechanism is set out below.

3.1 Advection

The advection is the movement of dissolved solute with flowing groundwater at the seepage velocity in porous media. The advection is governed by the Darcy's law as it is the transport of the solute. Darcy's law states that the flow rate of water through soil from point 1 to point 2 is proportional to the head loss and inversely proportional to the length of flow path

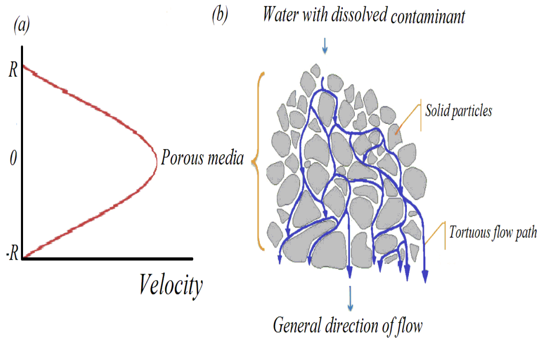

Fig. 1 Schematic diagram distribution of velocities in a single capillary (a) and distribution of velocities in a more complex pore system (b)

$$Q = -KA\frac{h_2 - h_1}{L} \tag{6}$$

Where Q is groundwater flow rate; A is cross section area of flow; h_2-h_1 is head loss; L is distance; K is hydraulic conductivity. The seepage velocity can be calculated as

$$v_a = -\frac{K}{n}\frac{h_2 - h_1}{L} \tag{7}$$

Where n is porosity.

3.2 Dispersion

It is the result of two processes-molecular diffusion and mechanical mixing. The mechanical mixing is results from the uneven distribution of water flow velocities within and between different soil pores (Fig. 1). Dispersion can be derived from Newton's law of viscosity which states that velocities within a single capillary tube follow a parabolic distribution, with the largest velocity in the middle of the pore and zero velocities at the walls (Fig. 1(a)). As soils consist of pores of many different radii, solute fluxes in pores of different radii will be significantly different, with some solutes again traveling faster than others (Fig. 1(b)).

The molecular diffusion is a process as a result of the random motion of chemical molecules. This process causes solute to move from a location with a higher concentration to a location with a lower concentration. Molecular diffusion can be represented by Fick's law as

$$F = -D_m\frac{\partial C}{\partial x} \tag{8}$$

Where F is mass flux; D_m is diffusion coefficient in unobstructed water media and $\frac{\partial C}{\partial x}$ is concentration gradient. The Fick's law was derived in unobstructed water solutions. When this law is applied to porous media, the diffusion coefficient should be smaller since the ions follow longer paths caused by the presence of solid particles and because of adsorption on solids. This application yields an apparent diffusion coefficient D^* represented by Charles *et al.* (1991)

$$D^* = \tau D_m \tag{9}$$

Where τ is tortuosity coefficient calculated by empirical equation which is expressed by Millington and Quirk (1961)

$$\tau = n^{1/3} \tag{10}$$

Since these two processes cannot be separated in groundwater flow, the coefficient of hydrodynamic dispersion is taken into account.

$$D_x = \alpha_L \frac{v^2{}_{ax}}{|v_a|} + \alpha_{TV} \frac{v^2{}_{az}}{|v_a|} + D^* \tag{11}$$

$$D_z = \alpha_L \frac{v^2{}_{az}}{|v_a|} + \alpha_{TV} \frac{v^2{}_{ax}}{|v_a|} + D^* \tag{12}$$

$$|v_a| = \sqrt{v^2{}_{ax} + v^2{}_{az}} \tag{13}$$

Where α_L is longitudinal dispersivity and α_{TV} is transversal dispersivity. Although conventional theory holds that α_L is generally an intrinsic property of the aquifer, it is found in practice to be dependent on and proportional to the scale of the measurement. Most reported values of α_L fall in a range from 0.01 to 1.0 time the scale of the measurement, the value of α_{TV} is typically 1/10 to 1/100 of the longitudinal dispersivity.

3.3 Sorption and degradation

Sorption is the exchange of molecules and ions between the solid phase and liquid phase, including adsorption and desorption. Adsorption is the attachment of molecules and ions from the solute to the solid phase causing a decrease of concentration of the solute this is called Retardation.

Desorption is the release of molecules and ions from the solid phase to the solute. The simplest form of the adsorption isotherm is the linear isotherm given by (Bear 1979)

$$S = K_d C \tag{14}$$

Where K_d is the distribution coefficient.

The degradation term is a general term and covers both radioactive decay and biodegradation. The general principle of the radioactive decay and biodegradation as well as their incorporation into the solute transport differential equation is defined such as a first order Kinetic reaction; thus, the rate of decay reaction clarifies such as below (Bear 1979)

$$r = \lambda R_d C \tag{15}$$

It should be noted that in the present research the sorption and degradation terms is ignored.

4. Numerical scheme

4.1 Numerical technique for flow equation

Two major grid generation approaches have been taken by the past investigators in the fields of finite-difference and finite-element methods. In the first approach, the solution domain is

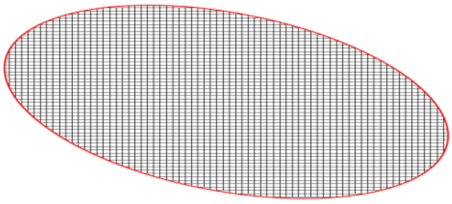

Fig. 2 Space discretization of the modeling domain

discretized using a fixed mesh (Desai and Li 1983). In this case, the solution domain should certainly involve the region where the seepage occurs therein. Since this approach performs many drawbacks, there have been many modifications to improve the accuracy of the approach. For example, Zhang *et al.* (2001) refine the distributed coarse grid suitably around the phreatic surface in order to improve the local accuracy of the solution. On the other hand, Holm and Langtangen (1999) take a similar strategy; however, they only focus on one node close to the phreatic surface to achieve the same accuracy benefiting from less computational trouble. The alternative approach is to choose moving grid (Chung and Kikuchi 1987), which has numerous superiorities comparing with the first approach. In this case, the solution domain is firstly guessed and a suitable mesh is filled in. The mesh size frequently changed during the solution procedure until determining the correct position of the phreatic surface.

In the present work, a structured quadrilateral mesh has been deployed to discretize the problem domain (Fig. 2). Scalar variables such as piezometric head are computed at the nodes which are placed at the centers of the cells and vector variables such as velocity are calculated at the intersection of grid lines.

The time splitting algorithm originally was proposed by Yanenko (1971) has been widely employed to solve numerically the governing partial differential equations. Employing this algorithm, the Boussinesq equation can be split into one double stage step as followings

$$S_s \frac{h^* - h^n}{\Delta t} = \frac{\partial}{\partial x}(K_x \frac{\partial h}{\partial x}) \tag{16}$$

$$S_s \frac{h^{n+1} - h^*}{\Delta t} = \frac{\partial}{\partial z}(K_z \frac{\partial h}{\partial z}) \tag{17}$$

In the stage one piezometric head at the previous time step n is used to diffuse in x direction to determine the new intermediate piezometric head h^*. In the second stage, using h^* to diffuse in z direction, the next step piezometric head, h^{n+1} is calculated. Implementation of finite volume on Eq. (17) makes

$$h_i^* = h_i^n - \frac{\Delta t}{\Delta x}(F_{i+1/2} - F_{i-1/2}) \tag{18}$$

$$F_{i+1/2} = -\frac{K_x}{S_s}(\frac{\partial h}{\partial x}) = -\frac{K_x}{S_s}(\frac{h_{i+1}^n - h_i^n}{\Delta x}) \tag{19}$$

$$F_{i-1/2} = -\frac{K_x}{S_s}(\frac{\partial h}{\partial x}) = -\frac{K_x}{S_s}(\frac{h_i^n - h_{i-1}^n}{\Delta x}) \tag{20}$$

F demonstrates the flux which, into or out of the system calculated as follows

$$F = -\frac{K}{\Delta t}\int_{t^n}^{t^{n+1}} \frac{\partial h}{\partial x} dt \tag{21}$$

This step uses the second order explicit scheme. It uses a classical iterative algorithm to obtain the solution of the free surface problem. This scheme is a fixed point algorithm, in which the free surface position is updated on each iteration on the basis of the comparison the computed piezometric head value with its elevation head until convergence is achieved. The cell is dried provided that the piezometric head value is less than the elevation head, in case the piezometric head value is greater than the upper cell elevation head, then the upper cell will be wetted. The cells are gradually dry or wet until reaching the correct phreatic surface. The drying and wetting may simultaneously occur during the solution procedure. The numerical simulation is carried out until steady-state condition is detected.

4.2 Numerical technique for transport equation

The present model uses a finite volume time splitting method to solve the transport equation in two steps. The first step, which is a double stage one, solves the diffusion terms in x and z directions to find intermediate concentrations C^{*}, C^{**}. In this step using the previous time concentration and the second order explicit scheme to find intermediate concentration.

$$\frac{\partial C}{\partial t} = \frac{\partial}{\partial x}(D_x \frac{\partial C}{\partial x}) \rightarrow \frac{C^{*} - C^{n}}{\Delta t} = \frac{\partial}{\partial x}(D_x \frac{\partial C}{\partial x}) \tag{22}$$

$$\frac{\partial C}{\partial t} = \frac{\partial}{\partial z}(D_z \frac{\partial C}{\partial z}) \rightarrow \frac{C^{**} - C^{*}}{\Delta t} = \frac{\partial}{\partial z}(Dz \frac{\partial C}{\partial z}) \tag{23}$$

In the second step, which is double stage too, using C^{**} and C^{***}.and the Fromm second order explicit scheme advection terms are calculated. The first stage is included solving advection in x direction using C^{**} to find the intermediate concentration C^{***} and the next stage is solving advection in z direction to find the next time concentration C^{n+1}.

$$\frac{\partial C}{\partial t} = -\frac{\partial (v_{ax} C)}{\partial x} \rightarrow \frac{C^{***} - C^{**}}{\Delta t} = -\frac{\partial (v_{ax} C)}{\partial x} \tag{24}$$

$$\frac{\partial C}{\partial t} = -\frac{\partial (v_{az} C)}{\partial z} \rightarrow \frac{C^{n+1} - C^{***}}{\Delta t} = -\frac{\partial (v_{az} C)}{\partial z} \tag{25}$$

Special techniques for solving advection-diffusion equations can be found in Namin (2003).

4.3 Initial and boundary condition

To obtain a unique solution of a partial differential equation, additional information about the physical state of the process is required. This information is supplied by initial and boundary conditions. For steady state problems, only boundary conditions are required, whereas for transient problems, boundary and initial conditions must be specified.

4.3.1 Initial condition

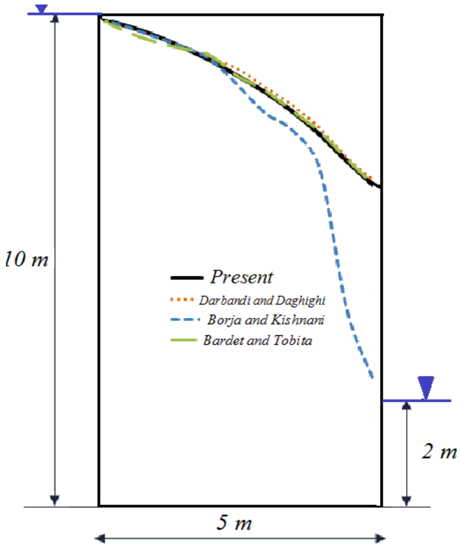

Fig. 3 The current phreatic surface solution and comparing Borja and Kishnani (1991), Bardet and Tobita (2002) and Darbandi and Daghighi (2007) model results

Since the flow model is obtained using an iterative algorithm, to start these iterations in the algorithm, an initial phreatic surface needs to be guessed. The solution of phreatic surface solves numerous unsteady situations, which is started with the initial condition and continue until adequately converges to steady state situation. Final solution won't be changed, despite using different initial conditions. In the transport model is a transient problem; as a result, initial condition plays an important role.

4.3.2 Boundary condition

Specifying conditions on the boundaries of a problem is one of the key components of a numerical analysis. Due to the extreme importance of boundary conditions, it is essential to have a thorough understanding in order to obtain meaningful results.

Boundary condition includes three types:

1. Head boundary condition
2. Specified boundary flow
3. Seepage face boundary

A constant-head boundary occurs where a part of the boundary surface of an aquifer system coincides with a surface of essentially constant head. In the type of specified-flux boundary, the flux across a given part of the boundary surface is considered uniform in space and can change with time. For seepage face boundary neither head nor flux is known. The pore pressure on a seepage face is zero.

5. Validation

Two test cases are now presented to verify the flow and transport solutions. The verification test cases consist of two-dimensional, groundwater flow and solute transport.

Table 1 Parameters of tests conditions

Material	Grain size (μm)	Velocity ($m/s \times 10^{-5}$)	Transverse dispersion coefficient ($10^{-9} m^2/s$)
Quartz	60-100	0.571	0.39

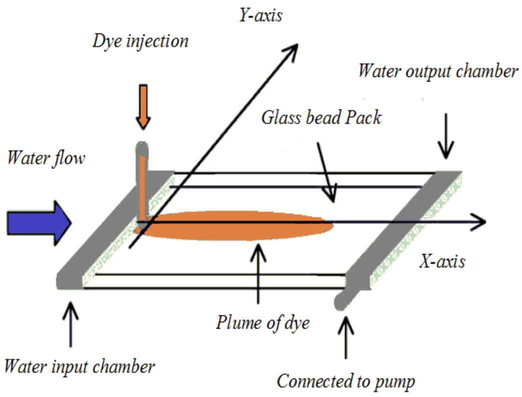

Fig. 4 Schematic of experiment setup

5.1 Validation of flow model

The developed flow formulation is validated against a test case. This case is an earthen dam with tail water investigated by Oden and Kikuchi (1980), Borja and Kishnani (1991), Lacy and Prevost (1987), Bardet and Tobita (2002), Darbandi and Daghighi (2007), As seen in Fig. 3, the width of the dam is 5 m and the reservoir elevation is 10 m. The Analytical solution which is used the Dupuit Forchhimer approximation won't be able to predict accurately the phreatic surface. The fact that the actual water table lies above the analytical one can be explained by the fact that, the Dupuit flows are all assumed horizontal, whereas the actual velocity of the same magnitude have downward vertical component so that a greater saturated is required for same discharge. At the downstream boundary a discontinuity in flow forms because no consistent flow pattern can connect a water table directly to downstream free water surface. The water table actually approaches the boundary tangentially above the water body surface and forms a seepage face.

Oden and Kikuchi (1980) use finite-element method and solve the problem for a fixed grid in the domain. The two other references use finite-difference method and trace the free surface by following some arbitrary pressure value. As is seen in Fig. 3, Borja and Kishnani (1991) do not predict the seepage face at all; the current formulation shows that the water is really seeping through the right face and the flow lines exit at atmospheric pressure. Comparing the present result with other results indicates that the current result is in good agreement with those of Bardet and Tobita (2002) and Darbandi and Daghighi (2007).

5.2 Validation of flow transport model

The second test case aims at validating the solute transport model. Experimental results obtained by Huang *et al.* (2002) were considered to compare with the simulation transport model results. The experiment was conducted in dimensions $180\times280\times10$ mm^3, its setup is shown in Fig. 4. This system can be evaluated as a 2D model, for its nominal thickness; therefore, the 2D

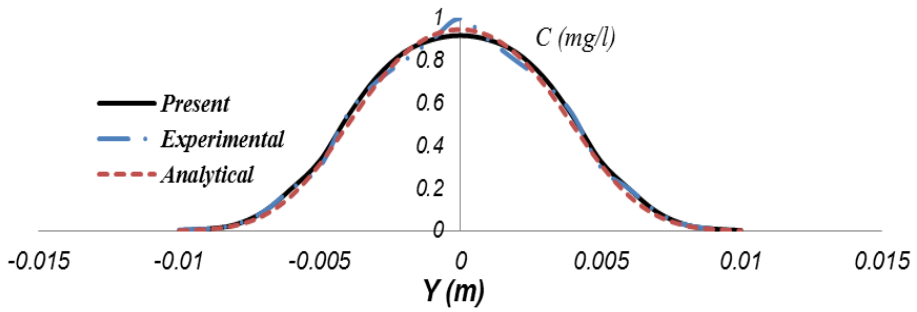

Fig. 5 Comparison of the experimental, numerical and analytical solution in section x=31 mm

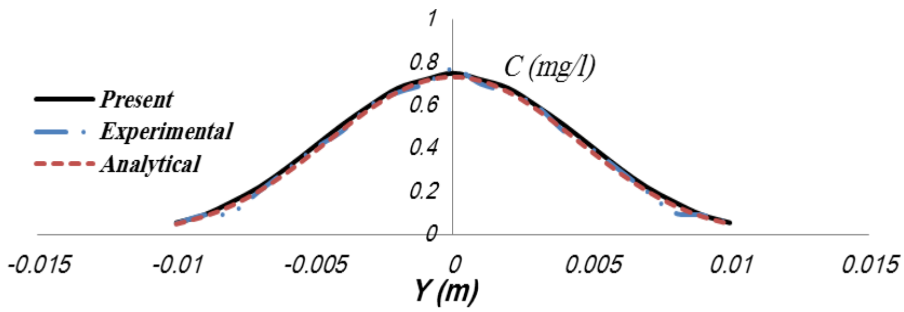

Fig. 6 Comparison of the experimental, numerical and analytical solution in section x=95 mm

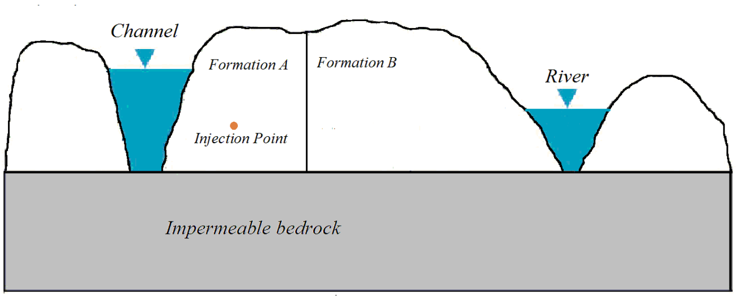

Fig. 7 Two dimensional domains of examples

dimensional experimental test case was carried out, the parameter of which are summarized in Table 1. The experiment was done for 24 hours. In the experimental test case, the contaminant distribution at two different sections with its analytical solution is reported. These results are compared with the numerical model and the comparison shows good agreement. (See Figs. 5 and 6). The maximum of relative error between experimental and numerical results equals 8.7% in the coordination of x=95, y=0 mm.

6. Model implementation

In order to study the effect and significance of soil parameters and stratification on the contamination migration some examples are considered. The example domain is a 2D vertical

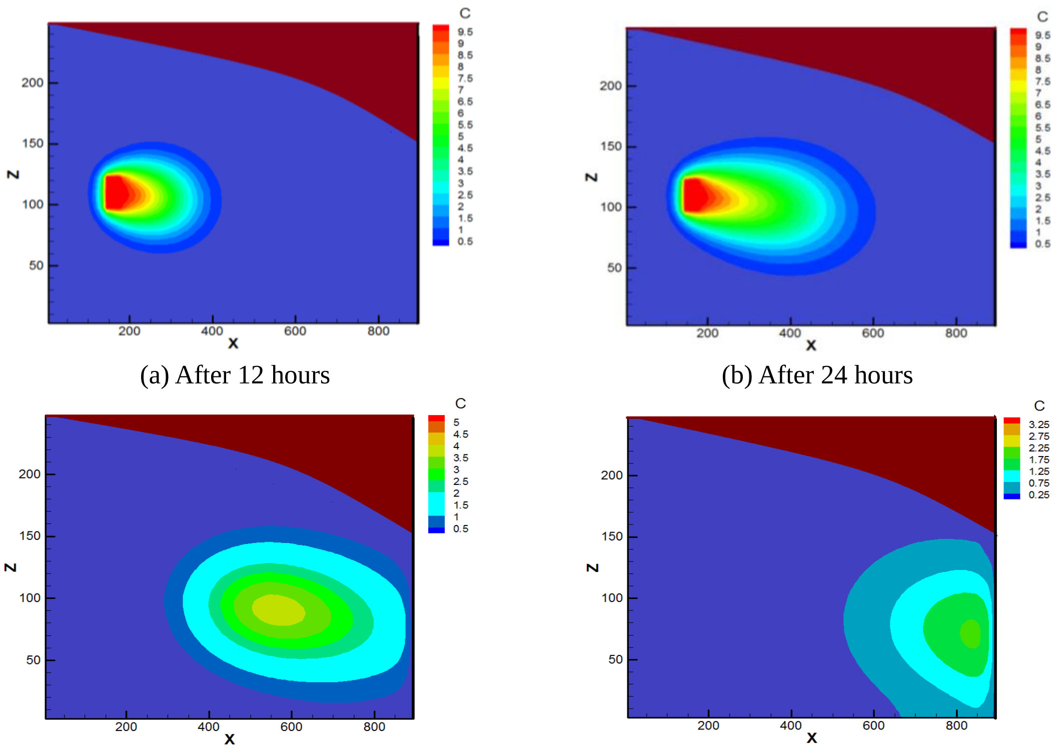

(a) After 12 hours (b) After 24 hours

(c) After 48 hours (d) After 72 hours

Fig. 8 Shape of solute plume in gravelly soil

having a length equal to 900 m in the *x* direction, a height of 250 m in the *z* direction with different configurations for the permeability and stratification (Fig. 7). The first formation properties are alike gravel. Its hydraulic conductivity, porosity and mean grain size respectively equal to 0.01 m/s, 0.3 and 10 mm. The second formation which is alike sand has the following soil properties hydraulic conductivity, porosity and mean grain size respectively equal to 0.0001 m/s, 0.45 and 1mm. The upstream and downstream heads equal to 250 and 150 m. Solute contamination is uniformly injected across in the coordination of *x*=150 m and *z*=110 m. The injection time is one day after that it will be stopped. Injection causes contaminant concentration to be 100 mg/l for 24 hours at injection point.

6.1 Example 1

In the first example configuration, the domain is composed of a homogeneous soil. The first case soil is gravel and the second one is sand. The concentration plumes over the simulation period in saturated gravelly and sandy region are evaluated in Figs. 8 and 9. Fig. 8 indicates advection in the permeable media is faster and the dispersion is slower. It is shown in the permeable region advection is prominent to the diffusion since in this region the seepage velocity has great value so its effect is much more significant. Inspection of the shape of the solute plume in Fig. 9 reveals that in region with lower hydraulic conductivity, advection effect decreases due to reduction of seepage velocity, on the other hand diffusion coefficient grows; thus, diffusion impact adds to.

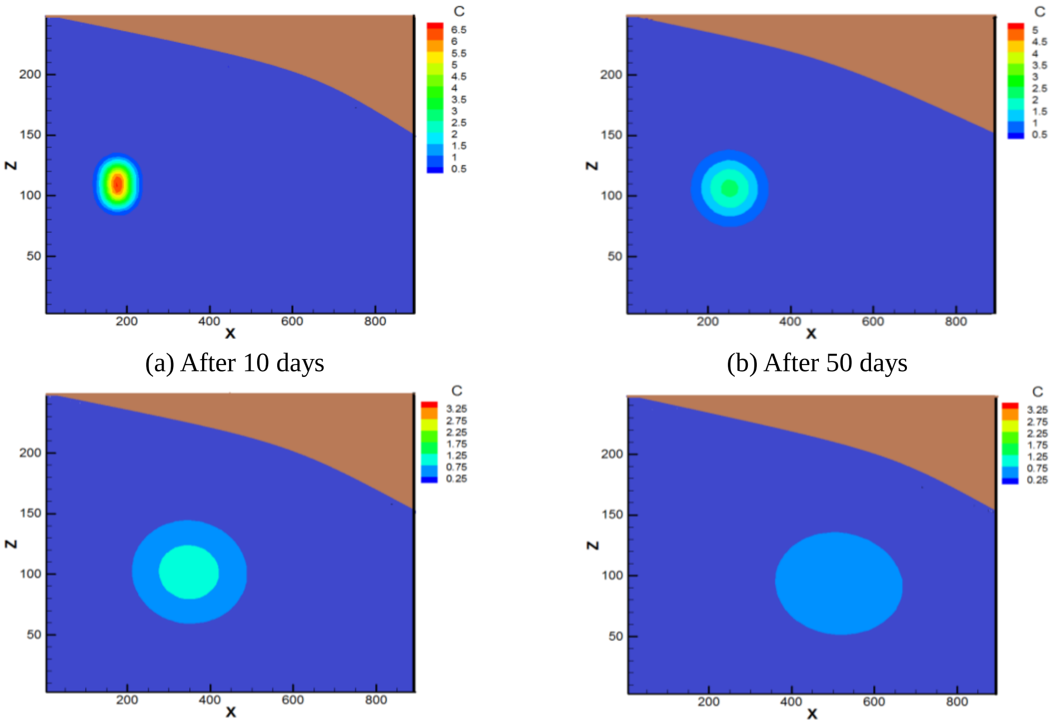

(a) After 10 days (b) After 50 days

(c) After 100 days (d) After 150 days

Fig. 9 Shape of solute plume in sandy soil

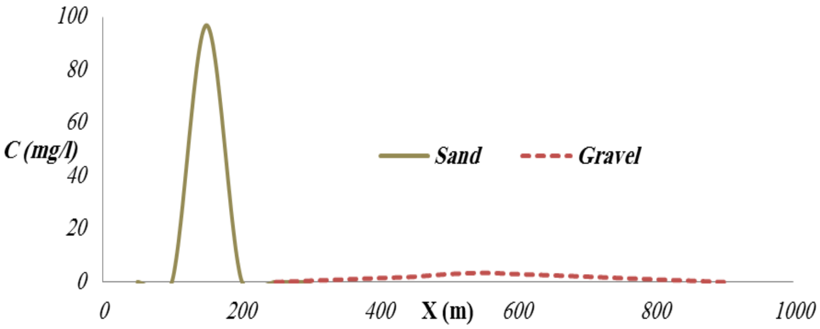

Fig. 10 Comparison of solute transport in gravelly and sandy soil after 2 days (z=105 m)

Comparison of contaminant migration in high and low permeable region can be seen in Fig. 10. The pollution in gravelly soil migrates quickly in regard to sandy soil and advection is dominating phenomena in the homogeneous gravelly media.

6.2 Example 2

Another simulation was carried out to investigate the effect of stratification and strata sequence in the porous media. The configuration of this example includes two strata with different permeability. The length of foremost strata is 300 m. The first case has two strata respectively

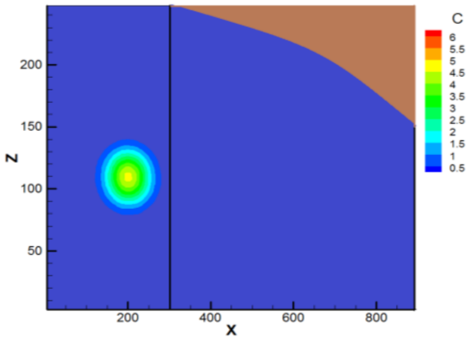

(a) After 10 days

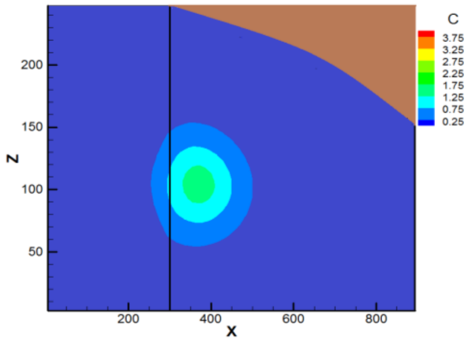

(b) After 60 days

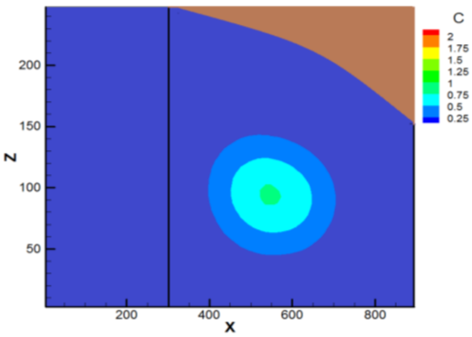

(c) After 120 days

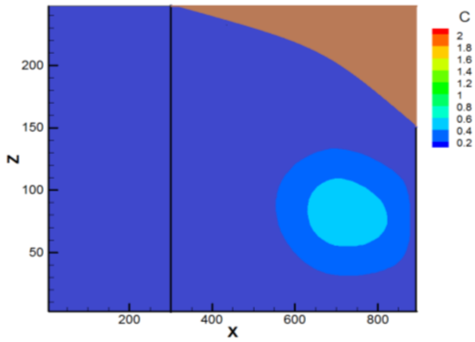

(d) After 180 days

Fig. 11 Shape of solute plume in G-S media

gravel and sand. Sequence of strata changes in second configuration case and starts with the sand. In Figs. 11 and 12 it can be seen that in the heterogeneous media Darcy velocity has relation to the height of seepage surface, this relation is interpreted by continuity equation. As the flow rate is constant, the region with less saturated area has the more Darcy velocity; however, it has the low hydraulic conductivity. Fig. 13 shows advection rate in the both strata is approximately constant. It is arise from the seepage velocity almost is equal in the both strata. Owing to continuity equation, Darcy velocity in the second stratum is greater and porosity of the second stratum is rather than the first. Consequently it leads to have the same seepage velocity in the both strata. On the other hand diffusion in the second strata boosts due to growth of diffusion coefficient. Fig. 14 indicates diffusion rate in the first strata is more in comparison to the second one; advection in the second stratum has much more importance than the first one, as a result further seepage velocity. The second stratum has the more Darcy velocity and the less porosity; thus, it makes the much more seepage velocity. It can be seen in Fig. 15 the advection and dispersion rate in the second case is more than the first; due to that the length of permeable formation is more.

6.3 Example 3

Another steady-state simulation was performed to investigate the effect of inclined lens on contaminant migration. The first configuration case is a sand lens, in gravel. The second one is gravel lens in sand. Fig. 16 indicates in a lower permeable lens reduces advection and increases

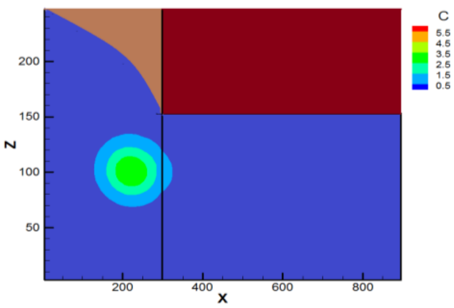

(a) After 10 days

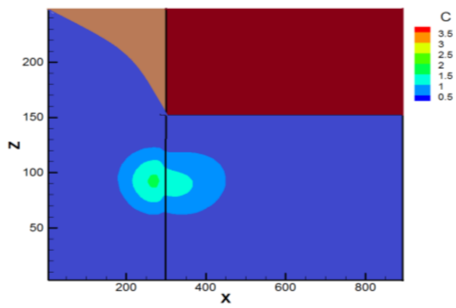

(b) After 20 days

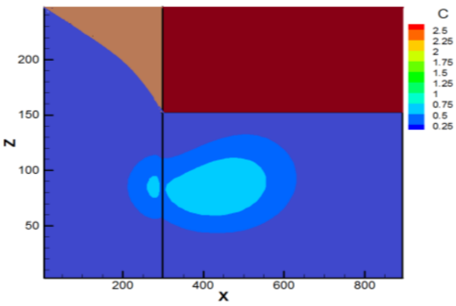

(c) After 30 days

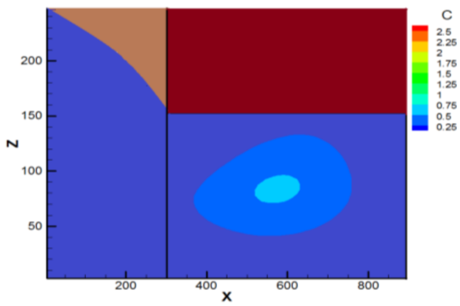

(d) After 40 days

Fig. 12 Shape of solute plume in S-G media

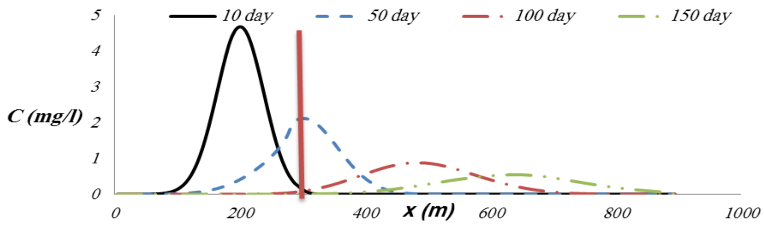

Fig. 13 Contaminant migration in G-S media (z=105 m)

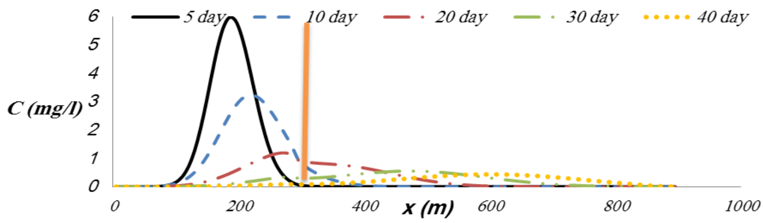

Fig. 14 Contaminant migration in S-G media (z=105 m)

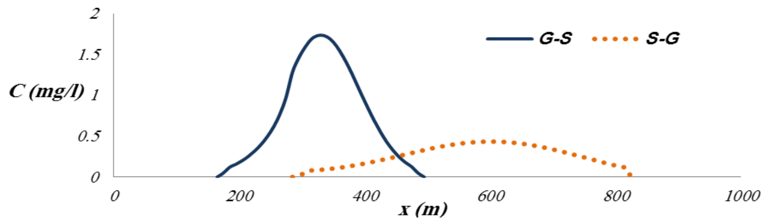

Fig. 15 Comparison of solute transport in G-S and S-G soil after 40 days

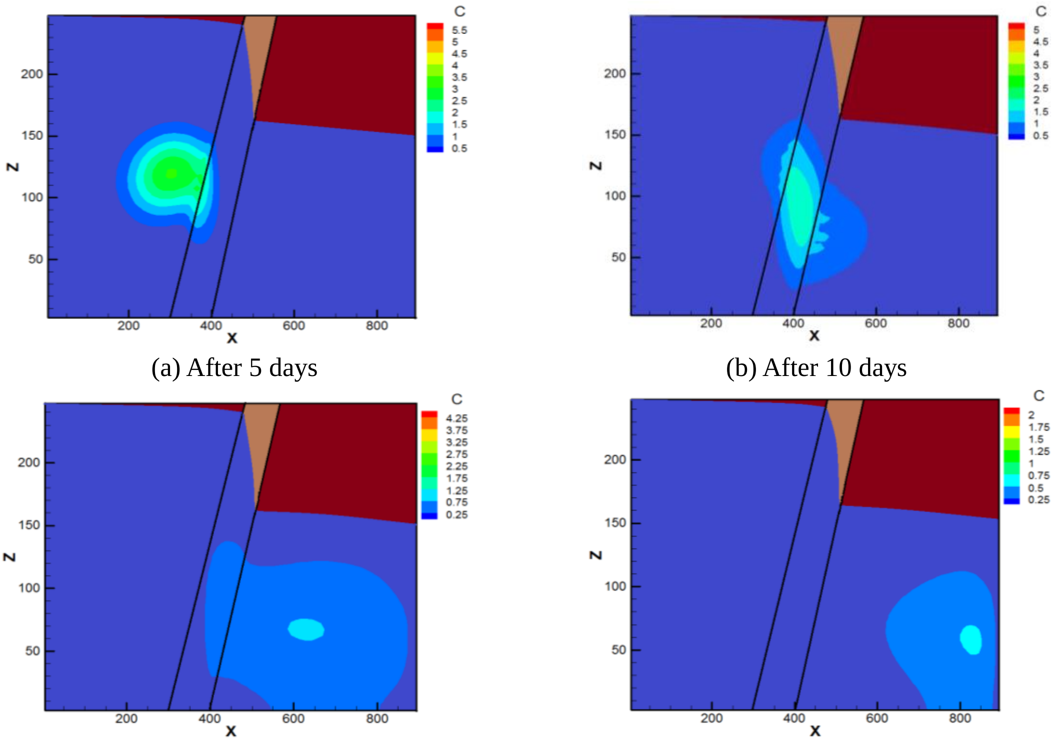

(a) After 5 days (b) After 10 days

(c) After 15 days (d) After 20 days

Fig. 16 Shape of solute plume in G-S-G media

diffusion so; it can impede or reduce the progress of contaminant in migration and the lens works as a barrier. Results of solute transport in sandy soil with a gravelly lens are presented in Fig. 17. According to this figure, diffusion reduces through the permeable lens and the inclined transition zone conveys solute plume downward, so acts as a drain. This example also shows that the present numerical model can predict and evaluate influence of containment on pollution migration.

7. Discussion

7.1 Discussion on example results

The results indicate that in homogeneous media, advection and diffusion respectively depend on seepage velocity and porosity. In permeable homogeneous media advection influence is more important than diffusion and by decreasing the hydraulic conductivity the significance of advection dwindle and diffusion emphasis expand. Compare to homogeneous media, advection depends on the height of seepage face and porosity, in heterogeneous media, in fact the less height of seepage surface represents the more Darcy velocity and the less porosity brings about the more seepage velocity. Diffusion in either homogenous or heterogeneous media just depends on porosity. The existence of different lens in homogeneous region plays a major role on solute transport. Low permeable lens reduces advection rate and diffuses contaminant through it.

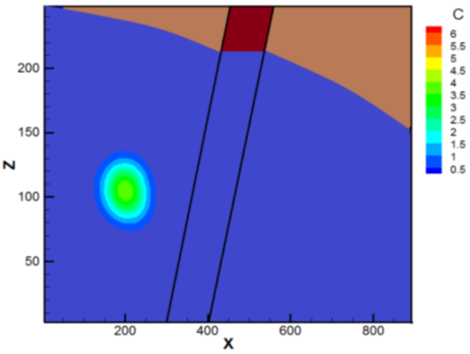

(a) After 20 days

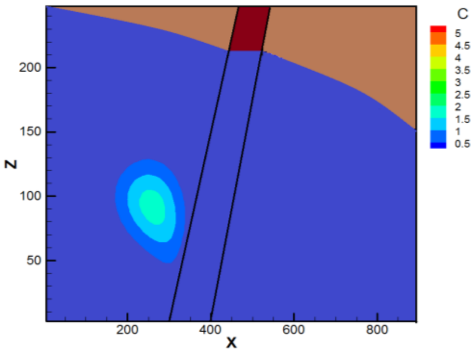

(b) After 50 days

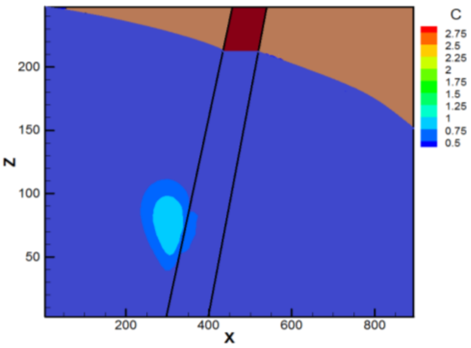

(c) After 80 days

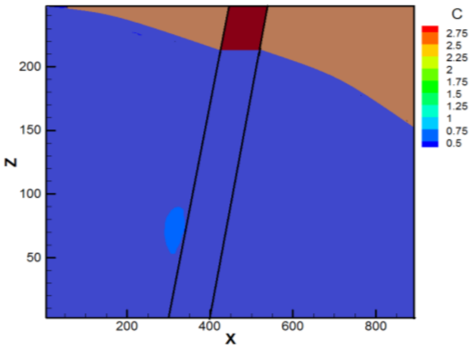

(d) After 110 days

Fig. 17 Shape of solute plume in S-G-S media

Consequently, it can stop or decline the contaminant migration. The lens with higher conductivity permeability increases the advection and decreases diffusion through it. Permeable lens direct contaminant downward and the contaminant plume get away from the groundwater table. In particular, the selection of the width of the lens and its soil properties such as its hydraulic conductivity and porosity plays a major role in controlling the solute transport in porous media.

7.2 The relative importance of the advection and diffusion in solute transport

As the governing Eq. (3) describe, the mass of solute transport through porous media is achieved by three different physical phenomena, namely advection, dispersion and diffusion. The share of which in the total flux has been taken here as a criterion to evaluate the importance of each phenomenon in the total transport.

Peclet number is a dimensionless parameter that indicates the relative importance of advection and diffusion to the transport scalars in a given system. This parameter is defined as below and it was investigated in examples as a criterion to evaluate the share of each phenomenon in contaminant transport equation.

$$Pe = \frac{Ud}{D_m} \tag{26}$$

Where U is seepage velocity; D_m is diffusion coefficient in unobstructed water media and d is

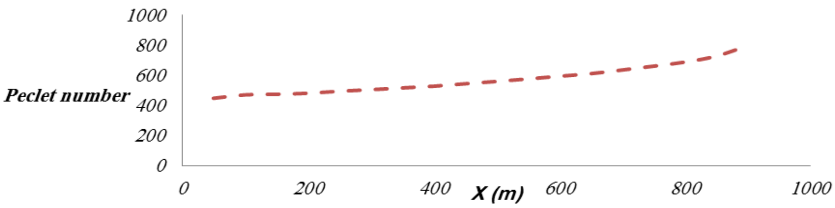

Fig. 18 Peclet number in gravelly soil (*z*=105 m)

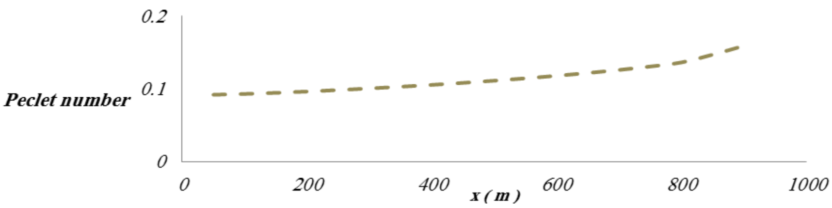

Fig. 19 Peclet number in sandy soil (*z*=105 m)

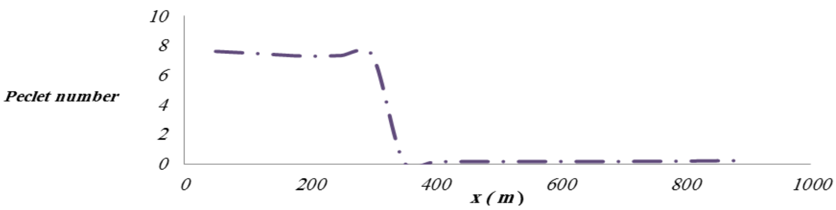

Fig. 20 Peclet number in G-S media (*z*=105 m)

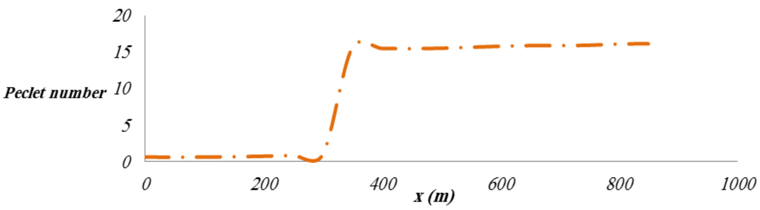

Fig. 21 Peclet number in S-G media (*z*=105 m)

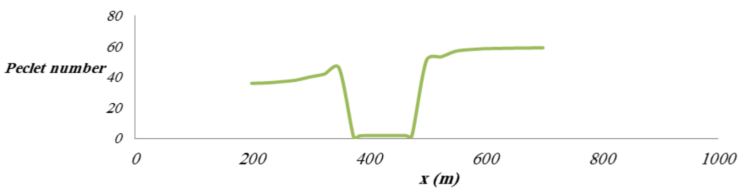

Fig. 22 Peclet number in G-S-G media (*z*=105 m)

grain size. Chunmiao and Gordon (1995) are show in the transport in porous media problem the value of Peclet number in the order of magnitude 6 and greater than that represent the relative dominance of advection and dispersion over diffusion.

Figs. 18 and 19 represent the Peclet number in the first example. There has been a gradual rise in the Peclet number due to the steady increment of the velocity in homogenous porous media. The Peclet number in homogeneous media with high permeability greater than the low one, which

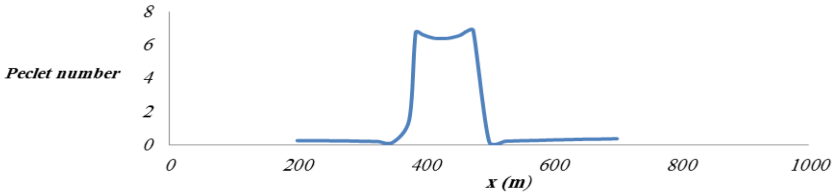

Fig. 23 Peclet number in S-G-S media (z=105 m)

means the ration of advection rate, is more.

The second example indicates the Peclet number of strata formation changes dramatically, so the relative importance of advection, dispersion and diffusion change too. Figs. 20 and 21 show the Peclet number drops quickly or climbs sharply on the strata formation. At the point of entering to lower permeable strata, it sharply declines and then levels off that are advection rate is reduced. At the point of entering to permeable strata, there is a sudden growth and then it remains constant.

Figs. 22 and 23 indicate a wildly fluctuating of Peclet number in the third example. The case which has lower permeable lens has a sharp drop at the point of entering to the lens and through that it is stable, after exiting, grows wildly and then levelled off. The case with the higher permeable lens has a sudden rise at the point of entering to the lens and through the lens, it is approximately constant, then after exiting, it has wildly reduction and then the recession has bottomed out.

8. Conclusions

To simulate solute transport in subsurface systems, groundwater flow and contaminant transport equations has been solved numerically by finite volume time splitting method in this research. The models can simulate the solute plume in layered soils with acceptable accuracy. Groundwater flow model extracted the phreatic line by iteration and the seepage velocities in the computational domain are derived from this model then, it is transferred to the transport model; thus, the saturated surface is selected for implementation of transport model. The transport model uses second order of accuracy to predict the fate of contaminant in layered soils. The accuracy of the flow and transport was demonstrated by favorable comparisons with experimental and analytical measurements. It also has been shown the influence of homogenous and heterogeneous regions on contaminant migration. Results show solute transport in homogeneous media depends on hydraulic conductivity and porosity, however; in heterogeneous media it depends on the height of seepage surface and porosity. Moreover; in low permeable region dispersion dominate still in high permeable media advection has the more importance in solute transport. Owing to the having negligibility of diffusion rate in the high permeable homogeneous media restoration will be more convenient in coarse graded soil regard to fine. It is notable that, the proposed model can develop better pre-emptive or remedial strategies and assess of aquifer clean up procedure among various methods such as pump and treat, in- situ treatment and containment.

References

Abolbashari, M.H. and Hosseini, M. (2016), “Generalized coupled non-fickian/non-fourierian diffusion-

thermoelasticity analysis subjected to shock loading using analytical method", *Struct. Eng. Mech.*, **60**(3), 529-546.
Bardet, J.P. and Tobita, T. (2002), "A practical method for solving free-surface seepage problems", *Comput. Geotech.*, **29**(6), 451-475.
Bear, J. and Cheng, A.D. (2010), *Modeling Groundwater Flow and Contaminant Transport*, Springer, New York, U.S.A.
Borja, R.I. and Kishnani, S.S. (1991), "On the solution of elliptic free boundary problems via Newton's method", *Comput. Meth. Appl. Mech. Eng.*, **88**(3), 341-361.
Boufadel, M.C., Suidan, M.T. and Venosa, A.D. (1999), "Numerical modeling of water flow below dry salt lakes: effect of capillarity and viscosity", *J. Hydrol.*, **24**(221), 55-74.
Charles, D. and Shackelford, D.E. (1991), "Diffusion in saturated soil", *J. Geotech. Eng.*, **12**,101-117.
Chung, K.Y. and Kikuchi, N. (1987), "Adaptive methods to solve free boundary problems of flow through porous media", *J. Numer. Analy. Meth. Geomech.*, **11**(1), 17-31.
Chunmiao, Z. and Gordon, D. (1995), *Applied Contaminant Transport Modeling*, Wiley, New York, U.S.A.
Darbandi, M. and Daghighi, Y. (2007), "A moving mesh finite volume method to solve free surface seepage problem in arbitrary geometries", *J. Numer. Analy. Meth. Geomech.*, **31**(14), 1609-1629.
Desai, C.S. and Li, G.C. (1983), "A residual flow procedure and application for free surface flow in porous media", *Adv. Water Res.*, **6**(1), 27-35.
El-Zein, A. (2008), "A general approach to the modeling of contaminant transport through composite landfill liners with intact or leaking geomembranes", *J. Numer. Analy. Meth. Geomech.*, **32**(3), 265-287.
Gallo, C. and Manzini, G. (2001), "A fully coupled numerical model for two-phase flow with contaminant transport and biodegradation kinetics", *Commun. Numer. Meth. Eng.*, **17**(5), 325-336.
Herrera, P. and Massabo, M. and Beckie, D. (2009), "A meshless method to simulate solute transport in heterogeneous porous media", *Adv. Water Res.*, **32**(3), 413-429.
Holm, E.J. and Langtangen, H.P. (1999), "A method for simulating sharp fluid interfaces in groundwater flow", *Adv. Water Res.*, **23**(1), 83-95.
Huang, W. and Smith, C., Lerner, D. and Thornton, S. (2002), "Physical modeling of solute transport in porous media evaluation of an imaging technique using UV excited fluorescent dye", *Water Res.*, **36**(7), 1843-1853.
Hulagabaly, A.M., Solanki, C.H. and Dodagoudar, G.R. (2014), "Contaminant transport modeling through saturated porous media using finite difference and finite element methods", *J. Mater. Civil Eng.*, **14**, 29-38.
Igboekwe, M. and Achi, N. (2011), "Finite difference method of modeling ground water flow", *J. Water Res. Protect.*, **3**, 192-198.
Jobson, H.E. and Harbaugh, A.W. (1999), "Modifications to the diffusion analogy surface-water flow model (daflow) for coupling to the modular finite-difference ground water flow model (modflow)", *U.S. Geological Survey Open-File Report*, 99-217.
Khoshghalb, A and Khalili, N. (2013), "A meshfree method for fully coupled analysis of flow and deformation in unsaturated porous media", *J. Numer. Analyt. Methods Geomech.*, **37**(7), 716-743.
Lacy, S.J. and Prevost, J.H. (1987), "Flow through porous media: a procedure for locating the free surface", *J. Numer. Analy. Meth. Geomech.*, **11**(6), 585-601.
Li, Y. and Cleall, P. (2011), "Analytical solutions for advective-dispersive solute transport in double-layered finite porous media", *J. Numer. Analy. Meth. Geomech.*, **35**(4), 438-460.
Millingtonan, J. and Quirk, P. (1961), "Permeability of Porous Solids", *Transac. Faraday Soc.*, **57**, 1200-1207.
Mousavi, N.M., Javadi, A.A., Al-Tabbaa, A. and Abbasi, F. (2011), "Stochastic finite element modelling of water flow in variably saturated heterogeneous soils", *J. Numer. Analy. Meth. Geomech.*, **35**(12), 1389-1408.
Namin, M.M. (2003), "A fully three dimensional non hydrostatic free surface flow model for hydro environmental predictions", Ph.D. Dissertation, Cardiff School of Engineering, Cardiff University, Wales, U.K.

Oden, J.T. and Kikuchi, N. (1980), "Recent advances: Theory of variational inequalities with applications to problems of flow through porous media", *J. Eng. Sci.*, **18**(10), 1173-1284.

Satavalekar, R.S. and Sawant, V.A, (2014), "Numerical modelling of contaminant transport using FEM and meshfree method", *Adv. Environ. Res.*, **3**(2), 117-129.

Sudicky, E.A. (1989), "The laplace transformation Galerkin technique: A time continuous finite element theory and application to mass transport in ground water", *Water Res. Res.*, **25**(8), 1833-1846.

Yaneko, N.N. (1971), *The Method of Fractional Steps,* Springer Verlag, New York, U.S.A.

Zhang, J., Xu, Q. and Chen, Z. (2001), "Seepage analysis based on the unified unsaturated soil theory", *Mech. Res. Commun.*, **28**(1), 107-112.

Zhang, Q., Volker, R.E. and Lockington, D.A. (2002), "Experimental investigation of contaminant transport in coastal groundwater", *Adv. Environ. Res.*, **6**(3), 229-237.

WL